Icarus 292 (2017) 48–53

Contents lists available at ScienceDirect

Icarus

journal homepage: www.elsevier.com/locate/icarus

Saturn's rings and associated ring plasma cavity: Evidence for slow ring erosion

W.M. Farrell[a,*], W.S. Kurth[b], D.A. Gurnett[b], A.M. Persoon[b], R.J. MacDowall[a]

[a] NASA/Goddard Space Flight Center, Greenbelt, MD 20771, USA
[b] University of Iowa, Iowa City, IA 011917, USA

ARTICLE INFO

Article history:
Received 7 May 2016
Revised 19 January 2017
Accepted 18 March 2017
Available online 21 March 2017

ABSTRACT

We re-examine the radio and plasma wave observations obtained during the Cassini Saturn orbit insertion period, as the spacecraft flew over the northern ring surface into a radial distance of 1.3 R_s (over the C-ring). Voyager era studies suggest the rings are a source of micro-meteoroid generated plasma and dust, with theorized peak impact-created plasma outflows over the densest portion of the rings (central B-ring). In sharp contrast, the Cassini Radio and Plasma Wave System (RPWS) observations identify the presence of a ring-plasma cavity located in the central portion of the B-ring, with little evidence of impact-related plasma. While previous Voyager era studies have predicted unstable ion orbits over the C-ring, leading to field-aligned plasma transport to Saturn's ionosphere, the Cassini RPWS observations do not reveal evidence for such instability-created plasma 'fountains'. Given the passive ring loss processes observed by Cassini, we find that the ring lifetimes should extend $>10^9$ years, and that there is limited evidence for prompt destruction (loss in <100 Myrs).

1. Introduction

On 1 July 2004, Cassini made the historic near-planet insertion burn placing it in orbit about Saturn, where it has been making fundamental discoveries of the planet's magnetosphere, ring, and atmosphere environment for the last 11 years. The Saturn Orbit Insertion (SOI) burn not only was a required planetary capture maneuver, but it also provided the Cassini science team with a unique close over-flight of the main (thick) rings, obtaining the first low energy plasma observations on field lines connected to the icy surfaces. Up to that date, no other spacecraft had passed closely over the rings with modern low energy magneto-plasma sensing instrumentation.

Unlike the Voyager flybys, Cassini's SOI occurred at southern summer when the planet and rings were at a relatively large tilt relative to the ecliptic, near 24°. As such, the southern facing portions of the rings were in direct sunlight while the northern facing portions of the rings where Cassini overflew were in relative shadow. Observations and modeling suggest that the UV sunlight on the southern rings dissociates molecules and atoms from the icy surfaces, and these low energy exospheric neutrals then ionize to form a ring exo-ionosphere in the ring's southern hemisphere (Young et al., 2005; Johnson et al., 2006; Bouhram et al., 2006; Luhmann et al., 2006; Tseng et al., 2010, 2011; Elrod et al., 2014; Persoon et al., 2015). In contrast, in the ring's northern, unlit hemisphere, the plasma content is anomalously low (assuming plasma neutrality over the B-ring, $<<1$ el/cm^3) (Gurnett et al., 2005; Xin et al., 2006) and this unexpectedly low plasma content is the primary focus of this paper.

While the two Voyager spacecraft did not fly directly over the rings, calculations at the time suggested meteoric impact at the rings would be the primary high energy source of plasma O and water ions along connecting flux tubes. Impact plasma flux levels emitted by the rings were estimated to be 10^9–10^{11}/m^2 s via micro-meteoroid weathering (Ip, 1983; Morfill et al., 1983) and such impact ionization events would be consistent with a steady-state plasma density of many 10′s per cubic centimeter (Plate 3 of Wilson and Waite, 1989). Further evidence of an active meteoric infall scenario was thought to be in the form of the observed spokes (Goertz and Morfill, 1983) which were suggested to be the visual near-surface manifestations of impact secondary ejecta (vapor, plasma, and dust).

Besides meteoric impact ionization, Northrup and Hill (1983) predicted that high q/m particles (ions, nanodust) inside of ~1.5 R_S, when displaced slightly from the ring plane, would develop a field-aligned force accelerating them away from the rings. They suggested this orbital instability would lead to charge particle loss from the rings, and suggested that this process accounts for the sharp and distinct drop in ring opacity at the B/C

* Corresponding author.
E-mail address: william.m.farrell@nasa.gov (W.M. Farrell).

http://dx.doi.org/10.1016/j.icarus.2017.03.022

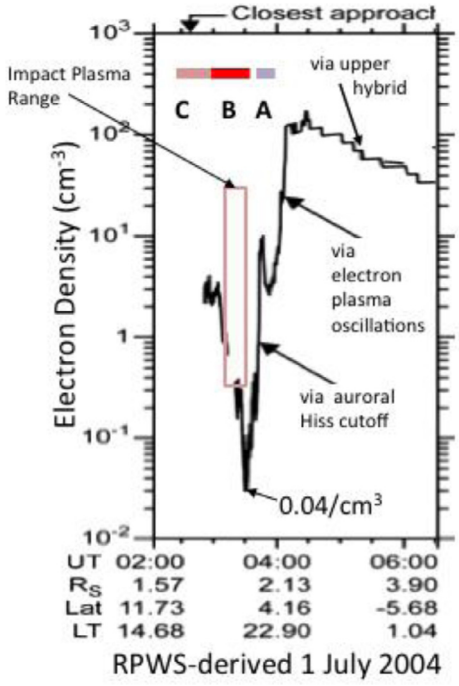

Fig. 1. The electron plasma density during Cassini's 1 July 2004 over-flight.

ring boundary. Thus, the Voyager era picture had the rings being vigorously eroded, becoming a source of plasma via meteoric impact ionization and the inner-ring particle instability, with the most intense impact plasma generated over the thickest part of the central B-ring (Wilson and Waite, 1989) and a possible dynamic field-aligned ion fountain expected over the C-ring (Northrup and Hill, 1983).

Our primary objective of this paper is to examine the Cassini SOI observations of the unexpectedly low plasma densities and juxtapose the observations to past predictions from Voyager studies. These past studies suggested more active, volatile ring surfaces vigorously eroded by continual micro-meteoroid impacts and affected by unstable plasma orbital dynamics inside of 1.52 R_s. We find a more passive ring environment that is suggestive of long ring life-times.

2. The plasma over the rings and the ring-plasma cavity

Cassini passed over the main rings from near 01:00 to just after 04:00 SCET on 1 July 2004. The primary thruster burn for SOI occurred from about 01:15 to 02:47 SCET and this thruster gas created very-low frequency (VLF) noise in excess of 30 dB, rendering a detection of the local electron plasma oscillation and upper hybrid emission difficult. However, from about 02:47 SCET onward, a near-continuous detection of the local electron density from discrete plasma wave tones was possible and is shown in Fig. 1 (adapted from Gurnett et al., 2005).

Specifically with the cessation of thruster noise, a strong emission at the local plasma oscillation frequency, $f_{pe} = 9000\, n_e^{1/2}$, was found, along with a whistler-mode auroral hiss emission in the center of the B-ring. The upper cutoff of this hiss is defined by the local f_{pe}. After 04:20 SCET, the local electron cyclotron frequency (derived from the magnetometer observations) became comparable to the electron plasma frequency, and intense narrowband plasma waves were detected at the local upper hybrid frequency $f_{uh} = (f_{ce}^2 + f_{pe}^2)^{1/2}$.

2.1. A-ring

Given these narrowband electrostatic wave modes and whistler-mode cutoffs, the associated electron density was derived (presented originally in Gurnett et al., 2005) and re-presented in Fig. 1. Note that just outside the A-ring (near 04:20 SCET), the electron densities peak at nearly 120 cm^{-3}, this in association with the local ionization of neutrals from Enceladus and the seasonal ring exo-ionosphere (Persoon et al., 2015). Re-examination of the Cassini CAPS ion spectrometer observations suggests ion densities in excess of 200–1000 cm^3 adjacent to the A-ring (Elrod et al., 2012, 2014). The ion content exceeds the electron content due to electron absorption onto small dust located in the ring plane (Johnson et al., 2017). A preliminary calculation of exo-ion mass loss onto the outer edge of the A-ring (~40 kg/s) was presented by Farrell et al. (2008). Their previous paper identified the mass loss as being primarily from the Enceladus torus. However, more recent works (Elrod et al., 2012, 2014; Tseng et al., 2013; Persoon et al., 2015) indicate that many of these neutrals and exo-ions observed adjacent to the A-ring during SOI may have originated from seasonal photolytic release from the inner main rings – thereby representing a dynamic redistribution of ring mass from inner to outer rings.

In association with this exo-ion mass loss at the A-ring (03:47-04:02 SCET), the electron density drops by nearly a factor of 40 to about 3 cm^{-3} in the center A-ring. While the rings appear to be absorbing the exo-ionosphere plasma, they are not perfect 'solid' absorbing boundaries. The optical depth in the central A-ring has a minimum of 0.4 (Esposito et al., 1983), and this optical porosity suggests a comparable electron porosity (or ring electron transmission through the central A-ring) of ~0.5. Hence, all electrons incident on these porous rings are not lost, and some fraction propagate between sunlit and shadowed hemispheres.

2.2. Cassini division

At the Cassini division between the A and B rings, the electron density has a local maximum approaching 10 cm^{-3} measured while the spacecraft was connected to field lines along the gap. This gap-plasma increase is associated with unobstructed field-aligned transport of sun-lit ring exo-ionosphere plasma from the ring's south side into the unlit northern region. Coates et al. (2005) reported that the electrons on field lines connected to the Cassini division possessed a warm population of ~5–10 eV electrons with peak densities near 1 cm^{-3}. However, due to spacecraft charging effects, the electron density may be an underestimate. If Cassini developed a negative potential of $\phi \sim 2\, kT_e/e$, the bulk of thermal electrons would not be detected by the Cassini electron spectrometer. Fortunately, the local electron plasma frequency is a very strong narrowband signal – the largest signal during this time period - allowing a supporting unambiguous measurement of n_e of 10 cm^{-3}. Cassini ion spectrometer observations found that corresponding ions in the gap are cool, near 1 eV (Young et al, 2005) with a density between 5–10/cm^3 (Bouhram et al., 2006; Elrod et al., 2012) thus providing an estimate for the local flux from the sunlit ring exo-ionosphere at $3 \times 10^{10}/m^2$ s.

High quality models by Bouhram et al. (2006) and Tseng et al. (2013) provide a contextual view of this ring exo-ionosphere: photo-ionization of neutral O_2 creates an enhanced plasma ion population that extends across the southern ring. These newly-minted ions in the Cassini Division can flow from the south sunlit side to northern unlit regions.

The ionization of neutrals emitted on the south sunlit side forms a season-dependent photolytic-driven low energy ring-ionosphere (Tseng et al., 2013). Tseng et al. modeled the photo-emitted neutrals from the dayside rings to be near 2×10^{27}/s or on

average at 10^{10}–10^{11}/m^2 s via photolytic processes and is a source of the exo-ionosphere and plasma in the Cassini division (Bouhram et al., 2006; Elrod et al., 2012).

2.3. B-ring

Before crossing the Cassini division, the spacecraft passed through field lines connected to the B-ring. As indicated in Fig. 1, the electron density had a substantial decrease or 'drop-out' with concentrations near 0.04 cm^{-3} in the central B ring near 1.7 R_s (Xin et al., 2006). Coates et al. show in their Fig. 5 that electrons over the B-ring are cold at thermal energies at or below 1 eV (Unfortunately, photoelectrons from sunlight through the C-ring affect CAPS electron observations acquired before 03:33 SCET). Elrod et al. (2012) analyzed the CAPS ion observations beyond 1.8 R_s, and found low densities values at 1.8 R_s of ~0.4 cm^{-1} which compare favorably with the RPWS measured electron plasma frequency at this location of ~ 6 kHz. The RPWS measurement of f_{pe} from the auroral hiss allows another independent measure of electron density over the B and C rings - extending the CAPS observations inward to lower radial distances. There is thus a distinct cold plasma cavity in the center of the B ring, with plasma densities at about a factor of 100 lower than in the adjacent A and C rings (which maintain a ~ 3–5 cm^{-3} density level in the central portion of these adjacent rings).

A key finding in this report is that the density in this ring-plasma cavity is substantially lower than those anticipated from Voyager-era estimates of impact-released plasmas. Wilson and Waite (1989) indicate that densities near 0.3 to 30 cm^{-3} should be expected in the central B-ring from impact plasma (represented by the pink shaded region on Fig. 1). Thus, the observation of this pronounced plasma cavity in the central B ring was unanticipated, if impactors were assumed to be driving the ring surface dynamics.

Xin et al. (2006) describe the ring plasma cavity as being analogous to the plasma cavities found in active auroral regions. Specifically in the center of this plasma cavity was the whister-mode auroral hiss emission often generated by a field-aligned electron beam. Such whister-mode auroral hiss emissions are naturally excited by the energetic electrons via the Cerenkov or electron cyclotron resonance – and the association of auroral hiss with field-aligned electron beams of moderate energy (0.1–10 keV) propagating through a magnetoplasma is nearly one-to-one (Farrell et al., 1988). Such electron beams are driven by field-aligned potential drops. As illustrated in Fig. 8 of Xin et al. (2006), the electron beam, auroral hiss, and plasma cavity are all believed to be part of a larger ring-generated current system driven by the change in angular momentum between the plasma-absorbing rings moving at Keplerian speeds and near-ring corotating plasma (for example, co-rotating plasma momentum is exchanged with the rings via surface absorption/capture of the newly-minted southern ring exo-ions that are also undergoing magnetic field pickup).

2.4. Electron density- ring opacity inverse correlation

Fig. 2 shows an RPWS wide band spectrogram of the VLF plasma waves observed during this ring over-flight. The electron plasma frequency is identified by the white line, and the lowest plasma frequency is found near 03:30 SCET near 1.7 kHz consistent with a 0.04 cm^{-3} density. The purple dots from 1.8 and 2.0 R_s are the electron plasma frequency derived using the CAPS ion density from Fig. 4 of Elrod et al. (2012), assuming plasma neutrality. Note that the independent methods arrive at similar values, especially for the low 0.4 cm^{-3} measured by both CAPS and RPWS near 1.8 R_s. The RPWS measurements extend further inward to <1.4 R_s. The inset in the figure is the ring optical transmission (optical depth from high to low value) derived from stellar occultation during the Voyager 2 mission (Esposito et al., 1983) overlaid to approximate scale. We find that the electron plasma frequency, and thus plasma density, appears to vary functionally-inversely with ring opacity from the A-ring to inside the C-ring. The inverse correlation is striking at the Cassini Division. Coates et al. (2005) initially reported this trend to be the case over the A ring and Cassini division – the outer portion of the main rings. Using the RPWS-derived electron plasma frequency herein, we find that this inverse trend between electron density and ring opacity continues inward over the B- and C-rings (as suggested by models (Bouhram et al., 2006; Tseng et al., 2013)).

As suggested in both Young et al. and Coates et al., if the northern electrons in shadow are generated from photo-ionization of ring exo-ionopshere on the southern sunlit side, they are required to propagate/penetrate through the porous rings to be detected in the unlit northern hemisphere by Cassini. In this scenario, one might anticipate an inverse trend in electron density and ring opacity, with the electrons from their southern source being effectively 'filtered' by the porous rings as they propagate along field lines into northern regions. An interesting future study would be to examine the nature of this ring-electron filter specifically considering whether a ring grain geometric cross-section or enhanced grain electrostatic cross section acts to form the barrier of the propagating electrons.

A key finding herein: The inverse relationship between topside low energy electron content and ring opacity would not be expected if impact processes dominated. For a quasi-uniform likelihood of impacts across the main rings, the greatest plasma concentrations via impact ionization would be expected where the largest amount of solid material is present –creating a direct relationship between electron content and ring opacity. The Cassini division would then be expected to generate the least amount of plasma along its connecting flux tubes, and the central B-ring the greatest plasma content (see Plate 3 of Wilson and Waite, 1989) - just the opposite of RPWS and CAPS (Coates et al., 2005) observations.

3. Enhanced ambipolar diffusion and constraints on the nature of 'ring rain'

The plasma pressure just over the central B ring is very low (e.g., as compared to outside the A ring) and the presence of the cavity should increase the ambipolar diffusion outflow from the ionosphere along the ring-to-ionosphere connecting field lines. In an analog to depleted flux-tubes in the terrestrial plasmasphere, the ionospheric plasma at the exobase becomes accelerated via ambipolar processes, thereby increasing outflows along the field lines to fill-in the low latitude evacuated plasma region. We might also expect some inward cross-B field diffusion from field lines connected to the more-dense A-ring but diffusion along the field line is expected to be faster.

Wilson and Waite (1989) developed a model of field-aligned plasma transport from the rings to the ionosphere, including ambipolar diffusion. They examined gravitational, magnetic mirror, centripetal and electrical forces acting on outflowing ionospheric light H^+ ions (outflow from exobase to higher altitudes) and energetic ring-generated O^+ plasma influx into the ionosphere exobase (inflow from rings into ionosphere and lower altitudes). They consider two cases for impact-generated ring plasma from the central B-ring: O^+ fluxes at 10^{11}/m^2 s (consistent with those required for water ring rain) and 10^9/m^2 s. For an impact ring plasma flux of 10^{11}/m^2 s, the ambipolar diffusion of the ionospheric population (H^+ at 10^4 cm^{-3}) is shunted on field lines beyond about 1.8 R_s. This cessation of ionospheric outflows is due to neutralization of the ambipolar potential above the exobase by the intense inflowing O^+ ring ions. However, for a weaker O^+ ring inflow at 10^9/m^2 s, the

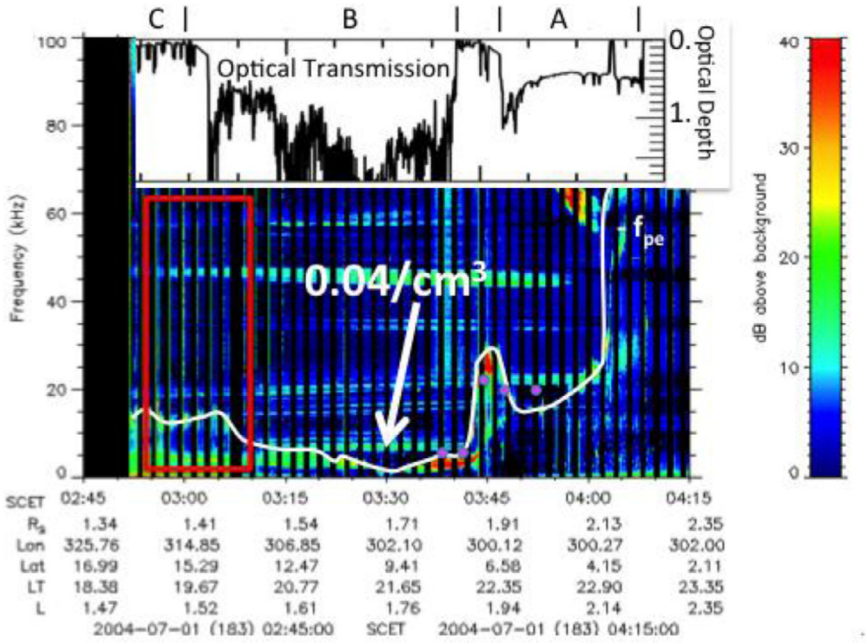

Fig. 2. A frequency versus time radio spectrogram showing the plasma emissions over the main rings as detected by the Cassini RPWS. The local electron plasma frequency is identified by the white line in the figure. The inset show an approximate comparison of the ring optical transmission (optical depth plotted from high to low value) from Esposito et al., 1983. Note that the electron plasma frequency varies inversely with ring optical depth. The dark purple dots between 03:37 and 03:52 SCET show the electron plasma frequency inferred from the CAPS ion densities (assuming plasma neutrality) measurements for comparison – adapted from Fig. 4 of Elrod et al. (2012).

ambipolar process remains strong across all field lines connected to rings, with ambipolar H^+ outflows a factor of 10 greater than the ring O^+ inflows into the exobase.

This study can be placed in context of our RPWS observations on the unlit ring surface: Observations of the B-ring plasma suggest a plasma flux that is a factor of 10 lower than the lower value used by Wilson and Waite (1989), near $10^8/m^2$ s (RPWS plasma density at 0.04 cm^{-3} and cool ion thermal velocity of 3 km/s (Young et al., 2005)). Consequently, at the Saturn ionosphere exobase, we expect the outflowing H^+ ionosphere flux to be close to a factor of 100 times that of the ring plasma inflow. While it has been suggested that ionospheric inflowing ring-originating water molecules may quench the ionospheric plasma by enhancing H_2^+ recombination rates, we find that water ions inflows connected to the unlit central B-ring and ring-plasma cavity are at levels at or below $10^8/m^2$ s, far lower than the levels necessary ($>10^{11}/m^2$ s) to substantially diminish the ionospheric peak density. If the rings are providing a water ion 'rain' into the ionosphere, we find it has to be very mild from the unlit northern surface or has to be in a form other than ions (possibly nano-sized particulates (Connerney, 1986; Connerney, 2013)).

Our inferences are in contrast to Voyager era modeling, but we do recognize that our findings are from a very limited ~4 h data set. While the SOI observations provide new insights, in 2017, Cassini will initiate the Proximal orbit sequence taking the spacecraft inside of the D ring and across flux tubes directly connected to the main rings – executing this transit over 20 times. A larger data set will be obtained to further constrain and identify the driving processes along the ring-connecting flux tubes.

As an example of the importance of the Proximal passages, O'Donoghue et al. (2013) reported on a reduction in the H_3^+ emission along field lines connected to the rings. This was interpreted at the time as quenching of H reactions due to the presence of ring-injected water into the ionosphere. However, an alternate interpretation is the possible decrease of H and its low mass molecular derivatives (H_2, H_3) via the enhanced ambipolar evacuation in the ionosphere due to the formation of the low pressure plasma cavity along these field lines. Hence, there may be multiple interpretations for the observed drop-out of H_3^+ emission. The upcoming Cassini Proximal passages should allow a unique in situ vantage point to search for any inflowing ring water gas & dust vs outflowing low mass species from enhanced ambipolar processes.

4. Inner edge of B-ring

Northrup and Hill (1983) analytically derived that high q/m particles (small dust and ions) may have unstable orbits inward of ~1.53 R_s. By comparing mirror forces to centrifugal and gravitational forces, any B-field parallel force would accelerate high q/m particles away from the equator. They suggest that mass loss via this instability is responsible for the low opacity C-ring and the sharp B/C ring boundary. Cassini passed directly over this region during SOI.

Fig. 2 shows the wideband waveform date from this region, with the red box identifying the B/C ring boundary region. We note that there is no unusual plasma density enhancement that might be expected from a fountain of high q/m ions driven along connecting magnetic field lines. As discussed in Northrup and Hill, an O^+ ion has q/m ~ 6×10^6 C/kg, and would be unstable to any off-plane displacement. By quasi-neutrality, we would anticipate the electron content to also increase and thus be detected by RPWS as an increase in local f_{pe}. However, such an increase is clearly not evident in the left hand portion of the spectrogram in Fig. 2.

We also did not find evidence of enhanced dust impacts that might be expected from micron-sized grains being accelerated along the field line. In Fig. 2, there are occasional broadband impulses on the spectrogram, but these are noise spikes associated with the change in mode of the wideband receiver. Comparable observations using the 10 kHz wideband mode does not reveal obvious evidence of an increase in impulsive dust grain impacts.

Admittedly, the Cassini RPWS is not sensitive to submicron and nano-sized grain impacts, and the loss of these particles cannot be

Table 1
A comparison of ring erosional processes describe in the literature. After the Cassini over-flight, photolytic processes are believed to be dominant at the ring surfaces.

Rate ($1/m^2$ s)	Authors[a]	Form[b]	Process	Ring lifetime (Gyr)
2×10^{13}	C&W	P, D	Max flux from unstable C-ring[c]	0.05
2×10^{11}	C&W	P, N, D	Impact flux needed for ring rain[d]	~4–5
1×10^{11}	W&W	P	Impacts	>5
3×10^{10}	T, X, F	P, N	Photolytic processes on sun-facing rings, Cassini division observations	>5
1×10^{9}	Ip, W&W	P, N	Impacts	>5
1×10^{8}	X, F	P	Ring plasma cavity observations	>>5

[a] C&W: Connerney and Waite, 1984; W&W: Wilson and Waite, 1989; T: Tseng et al., 2013; X: Xin et al., 2006; F: Farrell et al., This paper; Ip: Ip, 1983.
[b] P: Plasma, D: Dust, N: Neutrals.
[c] Max water flux expected from unstable region inside B-ring (see C&W).
[d] Main water flux needed to account for chemical loss of ionosphere H (see C&W).

determined. Also, Cassini passed over the northern portion of the rings, and the loss via the instability is expected to be largest in the southern hemisphere. However, there should still be a population of unstable ions, appearing as a 'fountain' of ions from the B/C ring boundary and C ring, on the northern side as well (see Fig. 2b of Tseng et al., 2013). Evidence for such an ion fountain is not observed in the corresponding electron density as detected by the RPWS plasma waves.

We conclude that the lack of the ion fountain and lack of substantial loss along the B-C ring boundary suggests some other inter-ring process, like local grain cohesion and/or electrostatics, is maintaining stability, offsetting the forces that create the instability and loss.

5. Conclusion

This set of SOI observations, together, point to a shift in thinking about space environmental ring loss (ring erosion): That it is not driven by an energetic impact process or instabilities, but instead is driven primarily by more passive photolytic processes (like that modeled by Tseng et al., 2013). At solstice, on dayside ring faces, photo-dissociation of neutrals and subsequent photo-ionization creates a passive exo-ionosphere, and Cassini RPWS and CAPS sampled this photo-ionized component during the overflight of the Cassini Division. On unlit faces, the electron absorbing rings determine the plasma content. The unlit side of the rings provide an opportunity to consider dominant processes when sunlight is 'turned off' (or at least the efficiency is way down): On these unlit sides, we find the electron plasma profile to be diametrically opposite to that expected from micro-meteoroid impacts, with the deepest loss of plasma in the densest portion of the B ring. We conclude, at least in this 4 hour SOI period, impact ionization is not driving the ring loss process on the unlit surface.

We present in Table 1 the ring loss flux and associated ring lifetime for a number of processes described previously, for comparison to those values herein. A maximum total erosion flux associated with the unstable portion of the rings (inward of B-ring) was presented as $2\times10^{13}/m^2$ s (Connerney and Waite, 1984). Such a flux would limit the inner ring lifetimes to <50 Myr.

In contrast, we find the losses via photolytic processes give rise to a solstice loss rates of $3\times10^{10}/m^2$ s on the sunlit face and a very low loss of $<10^8/m^2$ s on the unlit side. As modeled in Tseng et al. (2013) at equinox the photolytic losses become even lower, assuming unlit values on both ring faces. Given that intense impact and instability related plasma outflows are not observed by RPWS, we conclude that A-, B-, and C- ring lifetimes in the space environment can extend back to the formative periods of planet. Losses via the space environment will not limit ring lifetimes to the short 10′s of Myrs time scales.

We do recognize that our findings are from a very limited ~4 hour SOI data set and, in 2017, Cassini will initiate the Proximal orbit sequence taking the spacecraft across flux tubes directly connected to the main rings on >20 passages. Further insights on ring loss processes that define the ring lifetimes will be provided in this very exciting period. We do not exclude the possibility that ring erosional activity may be episodic – intensifying in meteoroid streams like those now recognized at our own Moon (Horanyi et al., 2015). Tiscareno et al. (2013) also suggested compact streams of particles can be incident on the rings. The multiple Proximal passes would extend temporal coverage beyond the limited but revealing SOI data set presented herein.

Acknowledgment

Research was funded via NASA's Cassini project.

References

Bouhram, M., Johnson, R.E., Berthelier, J.-J., Illiano, J.-M., Tokar, R.L., Young, D.T., Crary, F.J., 2006. A test-particle model of the atmosphere/ionosphere system of Saturn's main rings, Geophys. Res. Lett. 33, L05106. doi:10.1029/2005GL025011.
Coates, A.J., et al., 2005. Plasma electrons above Saturn's main rings: CAPS observations, Geophys. Res. Lett. 32, L14S09. doi:10.1029/ 2005GL022694.
Connerney, J.E.P., Waite, J.H., 1984. New model of Saturn's iono-sphere with an influx of water from the rings. Nature 312, 136–138.
Connerney, J.E.P., 1986. Magnetic connection for Saturn's rings and atmosphere. Geophys. Res. Lett 13, 773–776.
Connerney, J.E.P, 2013. Saturn's ring rain. Nature 496, 178–179.
Farrell, W.M., et al., 2008. Mass unloading along the inner edge of the Enceladus Torus, Geophys. Res. Lett. 35, L02203.
Farrell, W.M., et al., 1988. An analysis of the whistler-mode radiation from the Spacelab 2 electron beam. J. Geophys. Res 93, 153–161.
Elrod, M.K., Tseng, W.-L., Wilson, R.J., Johnson, R.E., 2012. Seasonal variations in Saturn's plasma between the main rings and Enceladus. J. Geophys. Res. 117, A03207. doi:10.1029/2011JA017332.
Elrod, M.K., Tseng, W.-L., Woodson, A.K., Johnson, R.E., 2014. Seasonal and radial trends in Saturn's thermal plasma between main rings and Enceladus. Icarus 242, 130–137.
Esposito, L.W., et al., 1983. Voyager photopolarimeter stellar occultation of Saturn's rings. J. Geophys. Res 88, 8643–8649.
Goertz, C.K., Morrill, G., 1983. A model for the formation of spokes in Saturn's ring. Icarus 53, 219.
Gurnett, D.A., et al., 2005. Radio and plasma wave observations at Saturn from Cassini's approach and first orbit. Science 307, 1255–1259. doi:10.1126/science.1105356.
Horanyi, M., et al., 2015. A permanent, asymmetrical dust cloud around the Moon. Nature 522, 324–326.
Ip, W.-H., 1983. On plasma transport in the vicinity og the rings at Saturn: a siphon flow mechanism. J. Geophys. Res 88, 819–822.
Johnson, R.E., et al., 2006. Production, ionization and redistribution of O2 Saturn's ring atmosphere. Icarus 180, 393–402. doi:10.1016/j. icarus.2005.08.021.
Johnson, R.E., et al., 2017. Nanograin density outside Saturn's A-ring. Astrophys. J. Lett. 834, L6.
Luhmann, J.G., Johnson, R.E., Tokar, R.L., Ledvina, S.A., Craven, T.E., 2006. A model of the ionosphere of Saturn's rings and its implications. Icarus 181, 465–474.
Morfill, G.E., Fechtig, H., Grun, E., Goertz, C.K., 1983. Some consequences of meteoroid impacts on Saturn's rings. Icarus 55, 439–447.
Northrup, T.G., Hill, J.R., 1983. The inner edge of Saturn's B ring. J. Geophys. Res 88, 6102–6108.

O'Donoghue, J., et al., 2013. The domination of Saturn's low-latitude ionosphere by ring rain. Nature 496, 193–195.

Persoon, A.M., Gurnett, D.A., Kurth, W.S., Groene, J.B., Faden, J.B., 2015. Evidence for a seasonally dependent ring plasma in the region between Saturn's A ring and Enceladus' orbit. J. Geophys. Res. Space Phys. 120, 6276–6285. doi:10.1002/2015JA021180.

Tiscareno, M.S., et al., 2013. Observtions of ejecta clouds produced by impacts onto Saturn's rings. Science 340, 460–464.

Tseng, W.-L., Ip, W.-H., Johnson, R.E., Cassidy, T.A., Elrod, M.K., 2010. The structure and time variability of the ring atmosphere and ionosphere. Icarus 206, 382–389. http://dx.doi.org/10.1016/j.icarus.2009.05.019.

Tseng, W.-L., Ip, W.-H., 2011. An assessment and test of Enceladus as an important source of Saturn's ring atmosphere and ionosphere. Icarus 212, 294–299. http://dx.doi.org/10.1016/j.icarus.2010.12.003.

Tseng, W.-L., Johnson, R.E., Elrod, M.K., 2013. Modeling the seasonal variability of the plasma environment in Saturn's magnetosphere between main rings and Mimas. Planet. Space Sci. 77, 126–135.

Wilson, G.R., Waite Jr., J.H., 1989. Kinetic modeling of the Saturn ring-ionosphere plasma environment. J. Geophys. Res. 94, 17287–17298.

Xin, L., Gurnett, D.A., Santolık, O., Kurth, W.S., Hospodarsky, G.B., 2006. Whistler-mode auroral hiss emissions observed near Saturn's B ring. J. Geophys. Res 111, A06214. doi:10.1029/2005JA011432.

Young, D.T., et al., 2005. Composition and dynamics of plasma in Saturn's magnetosphere. Science 307, 1262–1266.